Applied Physics Letters

Fracture toughness of radiation-damaged zircon studied by nanoindentation pillar-splitting

Cite as: Appl. Phys. Lett. **119**, 231903 (2021); https://doi.org/10.1063/5.0070597
Submitted: 08 September 2021 • Accepted: 27 November 2021 • Published Online: 08 December 2021

Tobias Beirau, Edoardo Rossi, Marco Sebastiani, et al.

ARTICLES YOU MAY BE INTERESTED IN

Grain-size dependence and anisotropy of nanoscale thermal transport in MgO
Applied Physics Letters **119**, 231604 (2021); https://doi.org/10.1063/5.0075854

Machine learning prediction of 2D perovskite photovoltaics and interaction with energetic ion implantation
Applied Physics Letters **119**, 231902 (2021); https://doi.org/10.1063/5.0072745

Perspective on statistical effects in the adhesion of micropatterned surfaces
Applied Physics Letters **119**, 230502 (2021); https://doi.org/10.1063/5.0073181

Fracture toughness of radiation-damaged zircon studied by nanoindentation pillar-splitting

Cite as: Appl. Phys. Lett. **119**, 231903 (2021); doi: 10.1063/5.0070597
Submitted: 8 September 2021 · Accepted: 27 November 2021 ·
Published Online: 8 December 2021

View Online Export Citation CrossMark

Tobias Beirau,[1,a)] Edoardo Rossi,[2] Marco Sebastiani,[2,a)] Warren C. Oliver,[3] Herbert Pöllmann,[1] and Rodney C. Ewing[4]

AFFILIATIONS

[1]Institute of Geosciences and Geography, Mineralogy/Geochemistry, Martin Luther University Halle-Wittenberg, 06120 Halle, Germany
[2]Engineering Department, "Roma TRE" University, Via della Vasca Navale 79, Rome 00146, Italy
[3]Nanomechanics Inc./KLA-Tencor, 105 Meco Lane, Oak Ridge, Tennessee 37830, USA
[4]Department of Geological Sciences and Center for International Security and Cooperation, Stanford University, Stanford, California 94305, USA

[a)]Authors to whom correspondence should be addressed: tobias.beirau@geo.uni-halle.de and marco.sebastiani@uniroma3.it

ABSTRACT

Nanoindentation micro-pillar splitting was employed to measure the fracture toughness (K_C) of growth-zones in radiation-damaged zircon with varying degrees of disorder (∼45%–80% amorphous fraction). The radiation-induced amorphization is caused by α-decay events from incorporated U and Th (∼0.22–0.43 wt. % UO_2 and ∼0.02–0.08 wt. % ThO_2). K_C has been found to increase with the increase in the amorphous fraction (∼2.39 to 3.15 $MPa^{*}m^{1/2}$). There is a good correlation with the modulus/hardness (*E/H*) ratio evolution over the investigated zones. As zircon has been proposed as a nuclear waste form for the incorporation and disposal of Pu, a deeper knowledge of K_C as a function of radiation damage is important, as radiation-induced cracking provides diffusion paths for the release of incorporated actinides. Zoned zircon provides a model for the development of multilayer coatings and complex ceramics that can be designed to be resistant to crack propagation.

Zircon ($ZrSiO_4$), a tetragonal nesosilicate mineral, is one of the most important minerals for geological age-dating (e.g., Ref. 1) and a potential nuclear waste host phase for the long-term incorporation and disposal of actinides, e.g., plutonium.[2–7] The zircon structure can incorporate high loadings of actinides, as Zr can be completely replaced by Th, U, Np, Pu, and Am.[2,8–17] Mainly due to the resulting α-decay of the incorporated actinides, the original atomic-scale ordering of the host structure undergoes a crystalline-to-amorphous transition (metamictization).[2,18] The structural damage results from atomic displacements (several thousand), caused by elastic collisions between the heavy recoil nucleus and surrounding atoms with each α-decay event. The recoil cascades within the periodic structure overlap with increasing fluence and result in an extremely disordered (metamict) state. The α-particle (helium nucleus) displaces only several hundred atoms at the end of its trajectory, losing most of its energy by electronic excitations. At least for zircon, percolation theory provides insight into the radiation-induced amorphization process.[19–23] In nature, zircon contains commonly up to 5000 ppm U and Th, while the total concentration can reach 10 wt. %.[4] As the ages of zircon often exceed 100 million years and the mineral has suffered radiation damage all over this time, it is an ideal natural material for which to investigate the long-term effects of intrinsic radiation damage on crystalline materials.[24,25] Murakami *et al.*[26] have provided a conceptual model of the evolution of the zircon structure with increasing radiation damage. As the structural amorphization of zircon leads to pronounced swelling and reduction in density,[14,21,26,27] a noticeable decrease in moduli and hardness has been observed.[22,23,28–32] An embrittlement of zircon has been observed by Ref. 31 with an increasing degree of crystallinity (less suffered radiation dose). In this context, micro-fracturing due to radiation-induced material swelling is an important point that has to be considered for durability estimates of crystalline and multiphase nuclear waste forms, as cracks can form pathways for radionuclide release from the host matrix.[33,34] Chakoumakos *et al.*[29,35] reported that fracturing (due to expansion of neighboring amorphous domains) was restricted to domains of higher crystallinity in a zoned zircon sample. The zoning is caused by variations in the distribution of incorporated U and Th. Although no direct measurements of the fracture toughness (K_C) have been made so far for zircon, it is assumed to increase with decreasing crystallinity.[29,35] As K_C is an essential material parameter required to understand the failure mechanism in detail, this Letter focuses on spatially resolved small-scale fracture toughness measurements of different growth zones with varying concentrations of U and Th that lead to a variation in the degree of radiation damage. The studied sample is a ~560 million years old,[36] well-characterized, natural oscillatory-zoned zircon specimen (#4601) from the Ratnapura district in Sri Lanka (for details, see Refs. 29, 32, 35, and 37: exactly the same sample was studied here and was stored safely in a padded thin section box, considering the already large sample age, no relevant changes should have occurred over the past few decades). Variations in the degree of structural disorder between different zones in this sample have been observed by transmission electron microscopy.[35,37] This zircon has micrometer-scale (001) zoning (~5–30 μm zones in width) as exposed in a (100) oriented polished thin section (0.03 mm in thickness). The studied area comprises around 10 zones with varying UO_2 and ThO_2 concentrations between ~0.22–0.43 wt. % and ~0.01–0.08 wt. %, respectively,[35] while each specific zone (see Fig. 1, zone alignments along the Y direction) comprises a relatively distinct and homogenous degree of structural disorder due to the suffered radiation damage by the α-decays of incorporated U and Th. The resulting suffered maximum lifetime alpha-decay event doses for the zoned area are displayed in Fig. 1 (calculated after Ref. 26).

Corresponding E/H values for the investigated zoned area have been calculated from nanoindentation high-resolution mapping data reported by Beirau *et al.*[32] (Fig. 1). Note, the inverse parameter (i.e., H/E) is an appropriate measure for the plasticity of an indentation.[38]

The nanoindentation micro-pillar splitting technique has been employed to measure the fracture toughness (for more details, see Refs. 39–42) of the different zones. In order to avoid biased results, transition regions were not taken into account. The micro-pillar splitting technique has been chosen, as fracture toughness has to be measured with a lateral spatial resolution below 20 μm, which excludes the use of conventional indentation cracking methods. The geometrical constraints of each zone limit the amount of possible applied load that is, in turn, required to induce cracking. The propagation of an eventually induced crack could be affected by the presence of the neighboring zones that would modify the nature and geometry of the crack system and possibly cause crack deflection at the interface. With pillar splitting, the probing volume is limited to that of the milled column, with no need of knowing the particular crack system. Substrate-induced artifacts are reduced since pillar splitting can occur at shallow indentation depths. Three to four micro-pillars [nominal diameter around 4 μm and an aspect ratio (height-to-diameter) $\geq$ 1] have been prepared in each zone by focused ion beam (FIB) milling (Fig. 1), using a previously developed preparation procedure that can minimize FIB-induced damage on the edge of pillars.[42] An early-stage multi-step milling for ring-core geometry machining of 0.28 nA has been employed at 30 kV acceleration voltage, followed by a final refinement at 48 pA to the nominal diameter of 4 μm, to further minimize ion-induced damaging. The incidence of the latter during pillar milling, indeed, was debated in related literature,[39–41] where it was found that it can be reduced to an altered thickness of ~100 nm for the usually

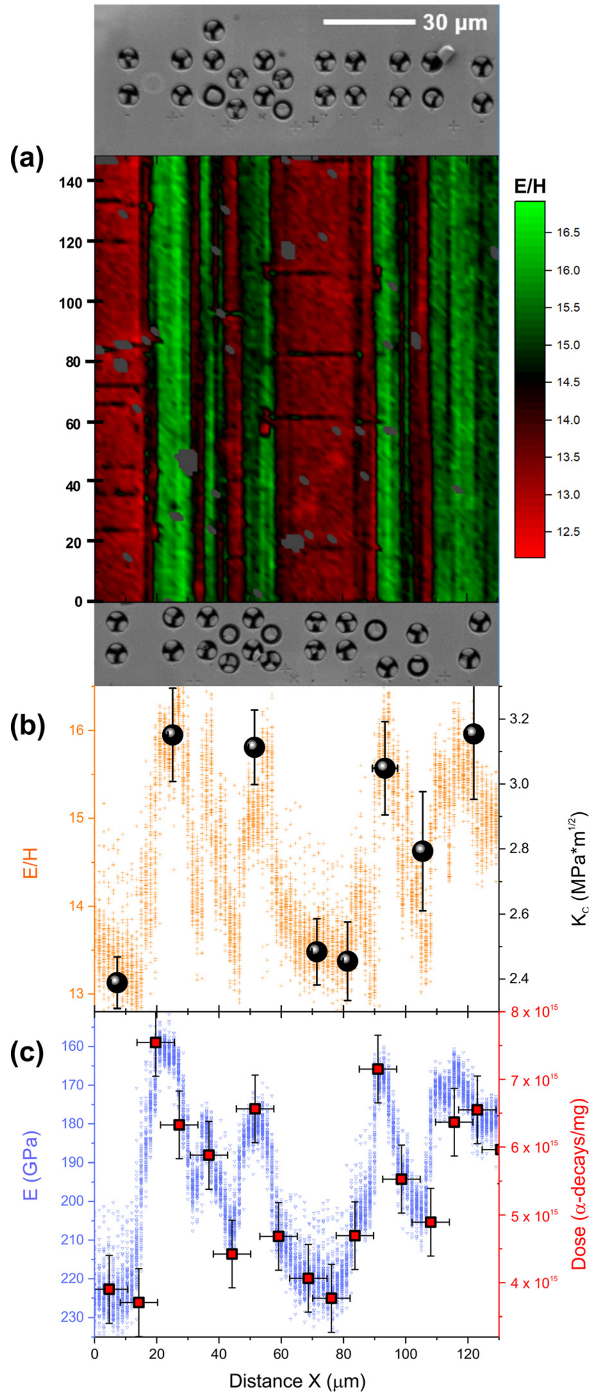

FIG. 1. (a) E/H mapping (E and H data from Ref. 32) of the investigated zoned area: higher crystalline zones (red) with horizontal cracks (darker features) and higher amorphous zones (green); areas where no data could be collected are in gray. Scanning electron microscopy micrographs of prepared micro-pillars in the zoned area after splitting (exact locations above and below nanoindentation mapped area are shown). Evolution of (b) E/H (orange crosses) and K_C (black closed circles) and (c) E (blue triangles) (data from Ref. 32) and dose (red squares) for the zoned area. X distance axis applies to whole Fig. 1.

adopted ion beam currents (below 0.28 nA). This considered, FIB damage becomes relevant only for pillar's diameters smaller than 1 μm and can be deemed as negligible for the present case. In a recent review article,[43] several micro-scale fracture testing geometries performances have been compared (e.g., cantilever beam) finding the pillar splitting as being the one allowing for the achievement of the lowest FIB damage artifacts. The aspect ratio of the pillars is larger than one, so they ensure full surface relaxation of the residual stress, if present.[44] Subsequently, a sharp indenter (diamond tip with a Berkovich geometry) is forced into the center of the pillar (constant strain rate of 0.05 1/s), which splits on attaining the critical splitting load (P_C) (burst in the load–displacement curve) (Fig. 2). From this, the fracture toughness can be computed by

$$K_C = \gamma \frac{P_c}{R^{3/2}}, \tag{1}$$

where R is the pillar radius and γ (see Table S1) is a calibration coefficient, while the latter was determined by cohesive-zone finite element modeling (CZ-FEM), considering the indenter geometry, crack propagation within the pillar, Poisson's ratio (ν), and elastic modulus/hardness (E/H) ratio.[39–42] The full range of γ values as a function of E/H values is given in a previous article.[41] The accurate positioning of the indenter at the center of each pillar was achieved by using a nano-positioning piezo-stage, which is available on a G200 KLA nanoindentation system. The used tip was fully calibrated on fused quartz reference sample, before and after each series of tests, according to ISO 14577 parts 1–3 standard.[45] K_C was averaged over the tested pillars in each specific zone.

The measured fracture toughness values show an excellent correlation with the variation of hardness (H) and modulus (E) (see Ref. 32) as well as their E/H ratio, over the different zones with varying degree of amorphization (Fig. 1). Observation of the splitting nanoindentation response curves for two representative zones (lower and higher E/H, respectively) (Fig. 2) shows the reproducible increase in the critical splitting load (P_C) as a function of the increment of E/H value with a direct correlation to increased toughness independently from the subsequent calculation of the γ coefficient (see Table S5). The comparison with the evolution of the elastic modulus (from Ref. 32) taken as a measure for the degree of crystallinity, as E is directly related to interatomic bonding, indicates an increase in K_C with increasing amorphization. An approximation of the amorphous fraction (f_a) of the measured zones can be made by comparing the average E value of the zone of interest (Fig. 1) with the E_{fa} evolution of the crystalline-to-amorphous transition in zircon obtained by mechanical modeling (see Ref. 23). This provides a range of ~45%–80% $\pm$ 5% amorphous fraction for the investigated zones. The highest degree of crystallinity and the most amorphous zone investigated in this study show K_C values of ~2.39 $\pm$ 0.08 and ~3.15 $\pm$ 0.2 MPa*m$^{1/2}$, respectively (Fig. 1). For comparison, a fracture toughness of ~1.7 MPa*m$^{1/2}$ for an undamaged zircon ceramic has been reported in literature.[46] Cracks have not been observed in or entering zones with E values $\lesssim$ 183 GPa,[32] corresponding to ~65% f_a[23] and a fracture toughness of ~3.11 $\pm$ 0.11 MPa*m$^{1/2}$.

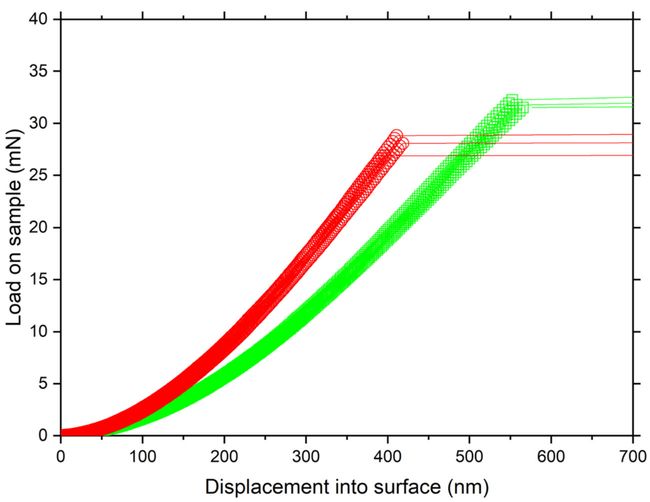

FIG. 2. Selected load on sample vs displacement into surface nanoindentation splitting curves of two representative zones at X distances (see Fig. 1) of ~7.3 μm (red circles, lower E/H and lower amorphous fraction) and ~25.1 μm (green squares, higher E/H and higher amorphous fraction).

As mentioned earlier, Chakoumakos *et al.*[29] reported (but did not measure) an increased fracture toughness of increasingly disordered zones. The microstructure of each zone can be assumed to comprise percolating crystalline and amorphous areas (as the first percolation point has already been exceeded for all investigated zones).[19–23] While the zones with the highest degree of amorphization are close to or have exceed the second percolation point (model dependent), where the crystalline parts cease to percolate and an amorphous matrix, surrounding isles of crystallinity, is established. Studies of Cm- or Pu-doped titanate phases also revealed an increase in fracture toughness with increasing radiation damage before the fully amorphous state is reached.[47–49] This behavior was attributed to internal strains induced by the composite nature of the structure.[48,50] Internal stresses have been reported as a possible mechanism of toughening.[51] In the case of the present work, relief of the cumulative contributions of Type II and Type III stresses[52] is ensured within the probing pillar volume due to the specific testing geometry.[39,53] Nevertheless, while these intertwined contributions are removed, the observed increase in toughness with increasing radiation damage (dose) might still be attributed to separate effects of internal strains associated with the defect enrichment of the preserved crystalline fraction and the overall increase in amorphized fraction (both cause swelling[26]) in the specific zones. The earlier described complex microstructure of radiation-damaged zircon is also influenced by the interfaces between the defect enriched crystalline domains and damaged amorphous regions.[22,23] While the latter is formed by overlapping recoil cascades, which consist of a densified outer layer populated by SiO_n polymers and an atomically depleted core (e.g., Refs. 54 and 55), therefore, one can assume the increase in stress, caused by increasing disorder, to raise the ability of the zircon structure to resist fracture, e.g., via crack-deflection mechanisms, i.e., a reduction in brittleness. Weak interfaces and other microstructural heterogeneities, influencing the overall elastic field, are reported to be able to deflect cracks, while second phases have found to allow for pinning and bowing of cracks.[51] It should be mentioned that Ref. 56 revealed by atomistic simulations, a brittle-to-ductile transition in quartz due to neutron-irradiation. They assumed that applying a load to the irradiated structure leads to dissipation of the accumulated energy by local self-organization, which induces plasticity.

In summary, a zoned zircon with a natural multilayered structure has been used to obtain insight into materials that comprise distinct regions with different degrees of brittleness, e.g., nuclear waste forms, and irradiated and further (partially) disordered phases. Precise fracture toughness measurements of a radiation-damaged zoned zircon, using the nanoindentation micro-pillar splitting technique, confirm [in the range of ∼45%–80% f_a, corresponding to a dose range of ∼0.18–0.29 displacements per atom (after Ref. 7)] the assumption of Chakoumakos *et al.*[29,35] of an increased K_C with increased f_a (from ∼2.39 to 3.15 $MPa^* m^{1/2} \approx 31.8\%$). This is in good agreement with the fracture behavior of other radiation-damaged phases (see above). These results also are consistent with chemically induced structural distortions and disorder that also can increase the fracture toughness of ceramics.[57] The self-irradiated zones, which display a decrease in brittleness (for the investigated f_a range) of zircon, provide a useful model for the development of multilayer coatings (e.g., superlattice films) and complex ceramics that are used in high radiation fields (e.g., designed for space applications). As zoned zircon represents a multilayered composite material with internal variations of comprised crystalline and amorphous fractions, one can draw a connection to glass-ceramics, where ZrO_2 is a common nucleation agent.[58,59] A sufficient way of synthesizing actinide-doped zircon has been proposed by, e.g., Ref. 60 using metallic zirconium, while a zircon ceramic can be prepared from pressed and fired ZrO_2 and SiO_4.[61]

See the supplementary material for details of the nanoindentation pillar-splitting experiments.

This research was funded by the Deutsche Forschungsgemeinschaft (DFG, German Research Foundation)—BE 5456/2-1 (T.B.). M.S. and E.R. gratefully acknowledge partial financial support from the European Commission, European project Oyster, Grant Agreement No. 760827.

FIB pillar preparation and nanoindentation pillar splitting were performed at the Interdepartmental Laboratory of Electron Microscopy (LIME), Università degli studi "Roma Tre," Rome, Italy.

AUTHOR DECLARATIONS

Conflict of Interest

The authors have no conflicts to disclose.

DATA AVAILABILITY

The data that support the findings of this study are available within the supplementary material.

REFERENCES

[1] D. W. Davis, T. E. Krogh, and I. S. Williams, Rev. Mineral. Geochem. **53**, 145 (2003).
[2] R. C. Ewing, W. Lutze, and W. J. Weber, J. Mater. Res. **10**, 243 (1995).
[3] W. J. Weber, R. C. Ewing, and A. Meldrum, J. Nucl. Mater. **250**, 147 (1997).
[4] R. C. Ewing, Proc. Natl. Acad. Sci. U. S. A. **96**, 3432 (1999).
[5] R. C. Ewing, Prog. Nucl. Energy **49**, 635 (2007).
[6] B. E. Burakov, Proc. Int. Conf. SAFE WASTE **93**, 19 (1993).
[7] W. J. Weber, A. Navrotsky, S. Stefanovsky, E. R. Vance, and E. Vernaz, MRS Bull. **34**, 46 (2009).
[8] C. Keller, Nukleonik **5**, 41 (1963).
[9] K. H. Walter, Ternäre Oxide des drei- bis- sechswertigen Americiums, Kernforschungszentrum Karlsruhe, Gesellschaft für Kernforschung M.B.H., Karlsruhe (1965).
[10] J. A. Speer, Rev. Mineral. Geochem. Orthosilicates **5**, 113 (1980).
[11] J. A. Speer and B. J. Cooper, Am. Miner. **67**, 804 (1982).
[12] W. J. Weber, J. Mater. Res. **5**, 2687 (1990).
[13] W. J. Weber, Radiat. Eff. Defects Solids **115**, 341 (1991).
[14] W. J. Weber, J. Am. Ceram. Soc. **76**, 1729 (1993).
[15] E. B. Anderson, B. E. Burakov, and E. M. Pazukhin, Radiochim. Acta **60**, 149 (1993).
[16] W. A. Deer, R. A. Howie, and J. Zussman, *Rock Forming Minerals: Orthosilicates* (The Geological Society, London, 1997).
[17] B. E. Burakov, J. M. Hanchar, M. V. Zamoryanskaya, V. M. Garbuzov, and V. A. Zirlin, Radiochim. Acta **90**, 95 (2002).
[18] R. C. Ewing, Nature **445**, 161 (2007).
[19] E. K. H. Salje, J. Chrosch, and R. C. Ewing, Am. Miner. **84**, 1107 (1999).
[20] K. Trachenko, M. T. Dove, and E. K. H. Salje, J. Appl. Phys. **87**, 7702 (2000).
[21] K. Trachenko, M. T. Dove, and E. K. H. Salje, J. Phys. **15**, L1 (2003).
[22] T. Beirau, W. D. Nix, R. C. Ewing, H. Pöllmann, and E. K. H. Salje, Appl. Phys. Lett. **112**, 201901 (2018).
[23] N. Huber and T. Beirau, Scr. Mater. **197**, 113789 (2021).
[24] R. C. Ewing and R. F. Haaker, Nucl. Chem. Waste Manage. **1**, 51 (1980).
[25] R. C. Ewing, B. C. Chakoumakos, G. R. Lumpkin, T. Murakami, R. B. Greegor, and F. W. Lytle, Nucl. Instrum. Methods Phys. Res. B **32**, 487 (1988).
[26] T. Murakami, B. C. Chakoumakos, R. C. Ewing, G. R. Lumpkin, and W. J. Weber, Am. Miner. **76**, 1510 (1991).
[27] H. D. Holland and D. Gottfried, Acta Cryst. **8**, 291 (1955).
[28] H. Özkan, J. Appl. Phys. **47**, 4772 (1976).
[29] B. C. Chakoumakos, W. C. Oliver, G. R. Lumpkin, and R. C. Ewing, Radiat. Eff. Defects Solids **118**, 393 (1991).
[30] E. K. H. Salje, Appl. Phys. Lett. **89**, 131902 (2006).
[31] T. Beirau, W. D. Nix, U. Bismayer, L. A. Boatner, S. G. Isaacson, and R. C. Ewing, Phys. Chem. Miner. **43**, 627 (2016).
[32] T. Beirau, W. C. Oliver, C. E. Reissner, W. D. Nix, H. Pöllmann, and R. C. Ewing, Appl. Phys. Lett. **115**, 081902 (2019).
[33] W. J. Weber and F. P. Roberts, Nucl. Technol. **60**, 178 (1983).
[34] W. J. Weber, J. Miner. Met. Mater. Soc. **43**, 35 (1991).
[35] B. C. Chakoumakos, T. Murakami, G. R. Lumpkin, and R. C. Ewing, Science **236**, 1556 (1987).
[36] A. Kröner, I. S. Williams, W. Compston, N. Baur, P. W. Vitanage, and L. R. K. Perera, J. Geol. **95**, 775 (1987).
[37] C. S. Palenik, L. Nasdala, and R. C. Ewing, Am. Miner. **88**, 770 (2003).
[38] H. Besharatloo and J. M. Wheeler, J. Mater. Res. **36**, 2198 (2021).
[39] M. Sebastiani, K. E. Johanns, E. G. Herbert, F. Carassiti, and G. M. Pharr, Philos. Mag. **95**, 1928 (2015).
[40] M. Sebastiani, K. E. Johanns, E. G. Herbert, and G. M. Pharr, Curr. Opin. Solid State Mater. Sci. **19**, 324 (2015).
[41] M. Ghidelli, M. Sebastiani, K. E. Johanns, and G. M. Pharr, J. Am. Ceram. Soc. **100**, 5731 (2017).
[42] C. M. Lauener, L. Petho, M. Chen, Y. Xiao, J. Michler, and J. M. Wheeler, Mater. Des. **142**, 340 (2018).
[43] J. Ast, M. Ghidelli, K. Durst, M. Göken, M. Sebastiani, and A. M. Korsunsky, Mater. Des. **173**, 107762 (2019).
[44] F. Archie, M. Z. Mughal, M. Sebastiani, E. Bemporad, and S. Zaefferer, Acta Mater. **150**, 327 (2018).
[45] W. C. Oliver and G. M. Pharr, J. Mater. Res. **7**, 1564 (1992).
[46] G. Suárez, S. Acevedo, N. M. Rendtorff, L. B. Garrido, and E. F. Aglietti, Ceram. Int. **41**, 1015 (2015).
[47] F. W. Clinard, Jr., D. S. Tucker, G. F. Hurley, C. D. Kise, and J. Rankin, MRS Proc. **44**, 664 (1984).
[48] W. J. Weber, J. W. Wald, and H. Matzke, J. Nucl. Mater. **138**, 196 (1986).
[49] W. J. Weber, R. C. Ewing, C. R. A. Catlow, T. Diaz De La Rubia, L. W. Hobbs, C. Kinoshita, H. Matzke, A. T. Motta, M. Nastasi, E. K. H. Salje, E. R. Vance, and S. J. Zinkle, J. Mater. Res. **13**, 1434 (1998).
[50] H. Matzke, Nucl. Instrum. Methods Phys. Res. B **32**, 455 (1988).
[51] B. Lawn, *Fracture of Brittle Solids*, 2nd ed. (Cambridge University Press, Cambridge, 1993).
[52] E. Salvati and A. M. Korsunsky, Int. J. Plast. **98**, 123 (2017).
[53] A. M. Korsunsky, M. Sebastiani, and E. Bemporad, Surf. Coat. Technol. **205**, 2393 (2010).

[54]I. Farnan and E. K. H. Salje, J. Appl. Phys. **89**, 2084 (2001).
[55]K. Trachenko, M. T. Dove, and E. K. H. Salje, Phys. Rev. B **65**, 180102 (2002).
[56]R. Ravinder, A. Kumar, R. Kumar, P. Vangla, and N. M. A. Krishnan, J. Am. Ceram. Soc. **103**, 3962–3970 (2020).
[57]C. Wang, L. Guo, Y. Zhang, X. Zhao, and F. Ye, Ceram. Int. **41**, 10730 (2015).
[58]P. Loiseau, D. Caurant, N. Baffier, L. Mazerolles, and C. Fillet, J. Nucl. Mater. **335**, 14 (2004).
[59]O. Dargaud, L. Cormier, N. Menguy, L. Galoisy, G. Calas, S. Papin, G. Querel, and L. Olivi, J. Non-Cryst. Sol. **356**, 2928 (2010).
[60]B. E. Burakov, E. B. Anderson, V. S. Rovsha, S. V. Ushakov, R. C. Ewing, W. Lutze, and W. J. Weber, Mater. Res. Soc. Symp. Proc. **412**, 33 (1995).
[61]M. Zhang, L. A. Boatner, E. K. H. Salje, R. C. Ewing, P. Daniel, W. J. Weber, Y. Zhang, and I. Farnan, Phys. Rev. B **77**, 144110 (2008).